PHYSOR-2006, ANS Topical Meeting on Reactor Physics
Organized and hosted by the Canadian Nuclear Society. Vancouver, BC, Canada. 2006 September 10-14

Study of CANDU Thorium-based Fuel Cycles by Deterministic and Monte Carlo Methods

A. Nuttin*[1], P. Guillemin[1], T. Courau[2], G. Marleau[3],
O. Méplan[4], S. David[5], F. Michel-Sendis[5], J. N. Wilson[5]

[1]*LPSC Grenoble (ENSPG), France*
[2]*EDF R&D Clamart, France*
[3]*École Polytechnique de Montréal, Canada*
[4]*LPSC Grenoble (UJF), France*
[5]*IPN Orsay (CNRS), France*

Abstract

In the framework of the Generation IV forum, there is a renewal of interest in self-sustainable thorium fuel cycles applied to various concepts such as Molten Salt Reactors [1,2] or High Temperature Reactors [3,4]. Precise evaluations of the U-233 production potential relying on existing reactors such as PWRs [5] or CANDUs [6] are hence necessary. As a consequence of its design (online refueling and D_2O moderator in a thermal spectrum), the CANDU reactor has moreover an excellent neutron economy and consequently a high fissile conversion ratio [7]. For these reasons, we try here, with a shorter term view, to re-evaluate the economic competitiveness of once-through thorium-based fuel cycles in CANDU [8]. Two simulation tools are used: the deterministic Canadian cell code DRAGON [9] and MURE [10], a C++ tool for reactor evolution calculations based on the Monte Carlo code MCNP [11].

KEYWORDS: CANDU, DRAGON, MCNP, bundle, once-through, thorium

1. Methodology and Study Roadmap

Our methodology consists in simple cell calculations that are representative of the average core, provided that a reactivity penalty accounts for the neutron leakage. Before considering more detailed simulations (with online refueling at channel level), this simple model will give us here first relevant indications on thorium use in CANDU. Results produced by the two simulation tools are cross-validated, thereby enhancing the confidence in both methods.

The first step is to model a CANDU-6 bundle loaded with U_{nat} fuel [12]. Mirror reflection boundary conditions are used to represent an infinite lattice of bundles. A burnup calculation is performed at a fixed average power. Once our methods at bundle level are validated on the U_{nat} case, we replace U_{nat} by short term available thorium-based fuels. The main goal is to identify some of the most interesting once-through options, that remain competitive compared to the U_{nat} cycle even without recycling the produced U-233 [8]. We investigate what could be the best combination of fissile starter (plutonium, slightly enriched uranium) and fuel spatial distribution. In particular, we compare Th/Pu fuel performance in CANDU and in PWR.

*Corresponding author, E-mail: nuttin@lpsc.in2p3.fr

2. Main Method Settings on U_{nat} CANDU-6 Benchmark

2.1 Description of our U_{nat} Bundle Model

CANDU-6 (power of 2000 MW_{th}, 700 MW_e) contains 380 channels of 12 bundles each. A bundle groups 37 fuel pins, moderated and cooled by D_2O [6]. For simplicity's sake, the slight moderator boron reactivity reserve used at start-up before first refueling, the reactivity control devices and the H_2O impurity in D_2O are not precisely simulated, but replaced by a constant 2000 pcm (20 mk) reactivity penalty [12]. During evolution, the bundle thermal power is kept constant at 450 kW. Nuclear data used are ENDF/B-VI (release 8) for MCNP and IAEA172 (the 172-group WIMS-D library recommended by the WLUP [13]) for DRAGON. For comparison on U_{nat}, we use ENDFB6 (172-group, from the WLUP) with DRAGON too. Temperatures are 300 K for steel vessel, moderator D_2O and Zircalloy-2 calandria tubes, 600 K for coolant D_2O, Zr-Nb pressure tubes and Zircalloy-4 fuel clads, and 1100 K for the fuel itself [14].

The simulated geometry is a fully mirrored CANDU-6 lattice square cell containing the fuel bundle surrounded by the moderator D_2O. At this bundle level, we do not take into account any axial flux dependence along the CANDU channel. We will thus consider the static flux level given by our mirrored calculation as an average of the different flux levels encountered over the axial trip occurring in reality. Another spatial discretization issue deals with the distribution of the fuel pins into 3 rings (7 inner, 12 intermediate and 18 outer pins), in order to take spectrum effects into account. We make the choice to always detail such 3 rings of fuel pins in our burnup calculations, based on an analysis performed with DRAGON showing that a correct evaluation of fuel burnup requires at least these 3 rings, while the use of 4 rings has no further impact.

Finally, we use with both methods the same optimized grid of time steps (corresponding to times for result editing in the EVO module of DRAGON and to MCNP calculations for new average cross sections in MURE). This grid consists roughly in 10-day steps until 50 days (very first steps are 1, 4 and 5 days), 20-day steps until 150 days and 50-day steps thereafter.

2.2 Comparison of U_{nat} Burnup Calculation Results

Figure 1: MURE and DRAGON U_{nat} bundle evolutions of k_∞, with the "plutonium peak".

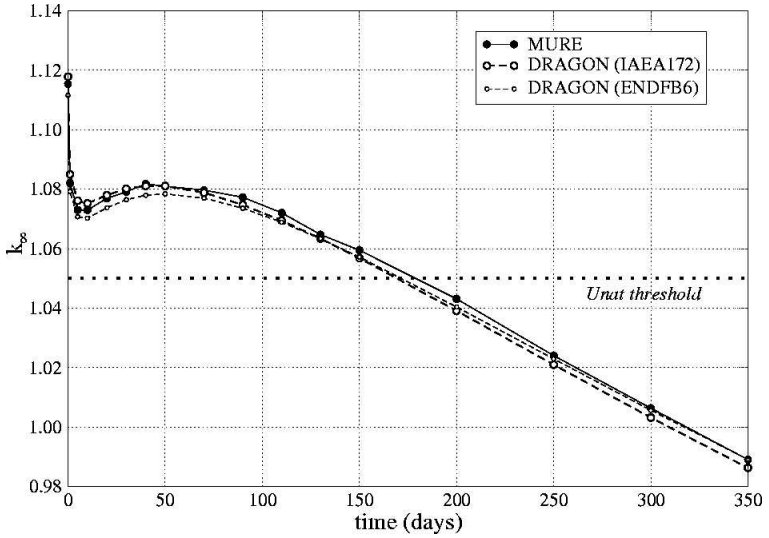

Figure 2: MURE and DRAGON (IAEA172) U_{nat} bundle evolutions of a few inventories.

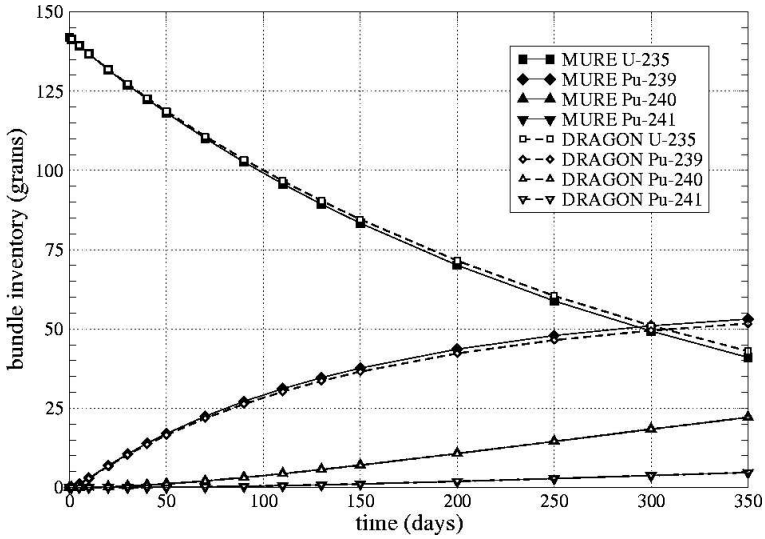

Figures 1 and 2 show a good agreement between DRAGON and MURE. The xenon saturation induces a very fast k_∞ drop in the first days. Typical of U_{nat} fuel, the "plutonium peak" is reached after about 50 days. It is due to the higher fission cross section of Pu-239 compared to U-235, which makes Pu-239 contribution to k_∞ increase temporarily faster than U-235 one decreases. Afterwards, k_∞ decreases at a rate imposed by the fission product poisoning, the U-235 exhaustion and the insufficient Pu-239 regeneration in CANDU thermal spectrum.

Maximal difference k_∞^{MURE} - k_∞^{DRAGON} (IAEA172) is about 400 pcm at 200 days. With fission products suppressed from bundle descriptions at the same time, this difference decreases to less than half (about 150 pcm), which identifies disparity in fission product treatment as a main cause for the relatively small k_∞ deviation between DRAGON and MURE. Let us note that differences due on one hand to methods (DRAGON/MURE) and on the other hand to nuclear data (IAEA172/ENDFB6 with DRAGON) are of the same magnitude.

2.3 Definition of the Cycle Irradiation Time

The bundle irradiation time can be deduced from a minimum on k_∞ corresponding to a k_{eff} value of 1, the difference including neutron leakage and not simulated absorptions. In order to evaluate the core neutron leakage, a simplified MCNP calculation is performed with a core entirely loaded with fresh U_{nat} fuel. The comparison between the bundle k_∞ and the core k_{eff} yields a total leakage (including vessel absorption) of about 2800 pcm. We check that leakage is always within 3000 pcm $\pm$ 500 pcm at other times, and use this value as a constant total leakage value for the U_{nat} core. Other methods for taking into account neutron leakage, such as buckling calculation or 3000 pcm moderator boron penalty, were tested with DRAGON. They all produced equivalent results in terms of reactivity and heavy nuclei inventory.

If we add the 2000 pcm reactivity penalty standing for non-simulated absorptions, we obtain $k_\infty^{threshold}$= 1.050 (so-called "U_{nat} threshold" on Figure 1) as approximatively constant threshold k_∞ bundle value corresponding to the full core criticality. Figure 1 gives us a so-called static bundle irradiation time T_{static} (defined by $k_\infty(T_{static}) = k_\infty^{threshold}$) of 170 days for DRAGON and 180 days for MURE. The corresponding burnup BU_{static}^{MURE} is 3500 MWd per metric ton of initial oxide fuel (MWd/tO from now on) at the chosen bundle power of 450 kW.

In order to compute the longer cycle irradiation time T_{cycle}, we have to take into account the compensation that occurs along a real channel of old bundle negative reactivity by new fed bundle positive reactivity. This is simply computed according to the following formula:

$$\frac{1}{T_{cycle}} \int_0^{T_{cycle}} k_\infty(t)\, dt = k_\infty^{threshold} \quad (1)$$

expressing that the associated k_{eff} is unity on average over T_{cycle} (corresponding to the bundle dwell time in its channel). Taking into account the benefits of the online refueling in such a way, the bundle cycle time T_{cycle} is found to be almost twice longer than T_{static} (T_{cycle}= 310 days for DRAGON, 330 days for MURE). The associated BU_{cycle}^{MURE} is 6400 MWd/tO, slightly below the reference value for average bundle exit burnup of 6600 MWd/tO (or 7500 MWd/ton of heavy nuclei [15]). The simple reason is that, as mentionned in part 2.1, we do not take into account the axial flux dependence along the channel. No significant sensitivity of T_{cycle} to nuclear data used (ENDFB6 instead of IAEA172 with DRAGON) has been noticed.

2.4 Analysis of the Main Reactivity Effects

We check here agreement between our codes on main reactivity coefficients of U_{nat} fuel at start-up. We focus on two important reactivity effects in CANDU: the Doppler coefficient for fuel temperature $\frac{\partial \rho}{\partial T})_{fuel}$ (pcm/K) and the Coolant Void Reactivity (CVR) $\Delta\rho_{void}$ (pcm). Doppler coefficient value at nominal fuel temperature (1100 K) is obtained by difference of reactivities at 1200 K and 1000 K. For Doppler calculations with MURE, we make MCNP runs long enough so that the Monte Carlo statistical errors are compatible with a chosen precision of 0.05 pcm/K (better would not be relevant because of nuclear data uncertainty common to both methods). CVR is computed ($\pm$ 10 pcm) by replacing the coolant nominal density of 0.8 g/cm^3 by zero. Table 1 shows good agreement on these effects, with well-known values [14].

Table 1: Main U_{nat} bundle reactivity effects at Beginning and End Of Cycle (BOC and EOC).

	@ BOC		@ EOC	
(DRAGON with IAEA172)	DRAGON	MURE	DRAGON	MURE
Doppler coefficient (pcm/K)	-1.07	-1.04	0.26	0.34
Coolant Void Reactivity (pcm)	1550	1690	1180	1270

Finally, a brief description of the positive contributions to CVR will help us to understand the corresponding values in thorium-fueled bundle studies. They can be partly listed following the well-adapted 4-factor decomposition of k_∞ [14] in a decreasing order of importance:

- Slowing down takes place only in moderator and thus epithermal resonance crossing is less probable in the fuel area (resonance escape probability p increases).
- Direct neutron paths from fission to fission are more probable without D_2O between fuel pins (fast fission factor ϵ increases).
- Suppressed coolant D_2O does not absorb neutrons anymore (thermal utilization factor f of neutrons in fuel increases).
- Thermal neutrons coming back from moderator cannot be heated up by coolant anymore, which makes cross sections (and reproduction factor η) increase.

3. Evaluation of a Few Options for Competitive Thorium Use

3.1 Homogeneous Th/Pu Bundle

3.1.1 Full Characterization for a Reference Plutonium

In all the following studies, the same model as that described in part 2 is used. The only WLUP library selected with DRAGON is ENDFB6. As a fissile starter mixed with Th-232 in a Th/Pu oxide fuel, we choose plutonium extracted after 5 years of cooling from the used UOX fuel of a N4 type PWR (Pu UOX from now on). Its isotopic vector is: 3.1, 52.5, 24.5, 12.2 and 7.7 mol% for Pu-238, Pu-239, Pu-240, Pu-241 and Pu-242 respectively [16]. We obtain an initial k_∞ of about 1.14 with a plutonium proportion in heavy nuclei of 2.0 mol%. We choose here a compromise between a classical reactivity management before first refueling (not too much extra reactivity reserve compared to the U_{nat} case) and a long enough cycle.

Figure 3: DRAGON and MURE Th/Pu bundle evolutions of k_∞, with two types of plutonium.

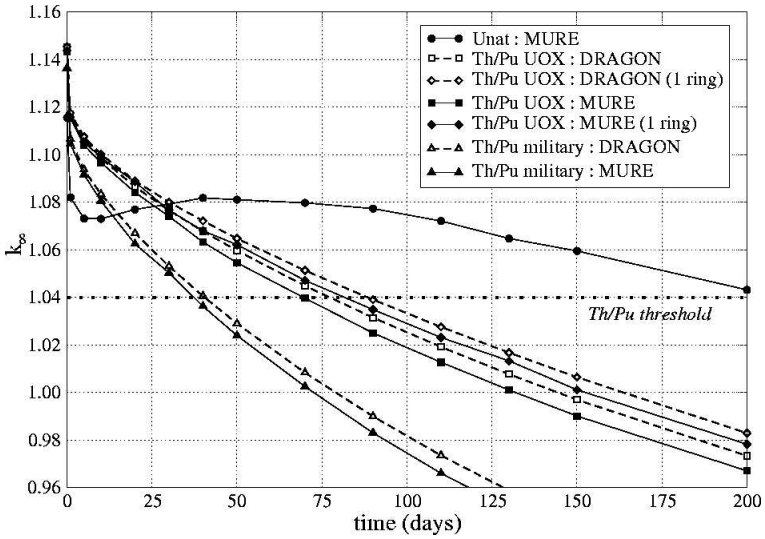

Figure 3 shows that k_∞ decreases more quickly with Th/Pu than with U_{nat} fuel. Produced fissile U-233 cannot compensate plutonium exhaustion as much as Pu-239 does for U-235 in the U_{nat} case. With a leakage penalty of 2000 pcm ($k_\infty^{threshold}$= 1.040), we obtain a Th/Pu UOX cycle time T_{cycle} of 170 days for DRAGON and 150 days for MURE. The corresponding burnup BU_{cycle}^{MURE} is 3200 MWd/tO (half the U_{nat} value). As a comparison, weapons-grade plutonium ("Pu military", 1.2 mol% in heavy nuclei for an initial k_∞ of 1.14) gives a smaller T_{cycle} with the same $k_\infty^{threshold}$ (90 days for DRAGON, 80 days for MURE) due to its low fertile contents (93, 6.5 and 0.5 mol% of Pu-239, Pu-240 and Pu-241 respectively). In the Th/Pu UOX case, Figure 3 shows that the k_∞ differences calculated by DRAGON and MURE between 1 ring and 3 rings are close, both reaching about 1000 pcm after 200 days. DRAGON and MURE evaluations of the spectrum effect between fuel rings are thus checked to be equivalent.

Table 2 gives the main reactivity effects of the Th/Pu UOX bundle at Beginning and End Of Cycle (BOC and EOC). Contrary to the U_{nat} case, the Th/Pu UOX bundle Doppler effect is still clearly negative at EOC. CVR values are lower than U_{nat} results, for the same reason that explains why U_{nat} CVR decreases with burnup; the fuel absorption rate increases compared to coolant (because of fission products and especially plutonium), which globally attenuates the positive CVR effects related to the factors f and η (as detailed at the end of part 2.4).

Table 2: Doppler and Coolant Void effects on the reactivity of the Th/Pu bundle.

(DRAGON with ENDFB6)	@ BOC		@ EOC	
	DRAGON	MURE	DRAGON	MURE
Doppler coefficient (pcm/K)	-0.54	-0.51	-0.24	-0.19
Coolant Void Reactivity (pcm)	870	970	990	1110

3.1.2 Comments on the Spectrum Effect Between Fuel Rings

Figure 4 emphasizes the strong spectrum difference between fuel rings. Due to its central location, the inner ring (7 pins) is the most distant from the moderator and obviously sees a less thermalized spectrum than the outer one (18 edge pins). We observe that the flux levels obtained are systematically lower in DRAGON (average fuel flux values of 1.64 10^{14} and 1.74 10^{14} n.cm^{-2}.s^{-1} for DRAGON and MURE respectively). The main reason is that MURE in its actual version takes 200 MeV as the fission energy released by any nucleus, while DRAGON uses isotope dependent Q-values from the library. This explains the flux level difference of about 5% (same relative deviation as that existing between U and Pu Q-values).

Figure 4: Normalized neutron energy spectra at start-up in CANDU Th/Pu inner and outer fuel rings (with total flux values in legends) by DRAGON (172 groups, left) and MURE (right).

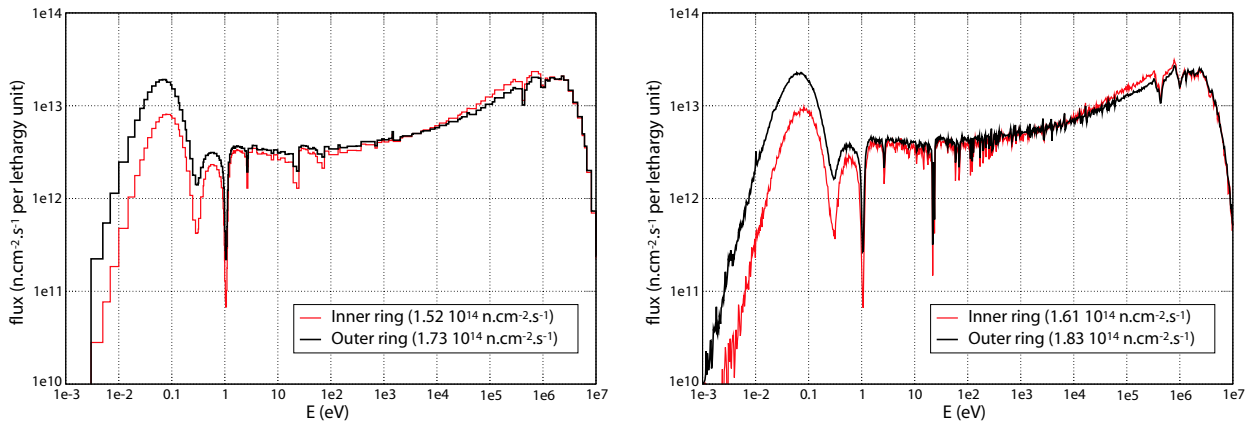

In terms of burnup, this spatial spectrum effect leads to much bigger differences on Pu-239 depletion between Th/Pu fuel rings that on U-235 depletion between U_{nat} fuel rings. Over a bundle cycle, the Pu-239 mass variation within the inner (outer) fuel ring of the Th/Pu bundle amounts to 0.58 (1.29) times the average mass variation in fuel, while the corresponding ratio for U-235 mass variation in the U_{nat} bundle amounts only to 0.84 (1.10).

3.2 Comparison with a PWR Th/Pu Assembly

3.2.1 Neutron Economy at Start-up

Burnup calculations of a 900 MWe PWR Th/Pu assembly have been made with MURE [5], with a constant thermal power of 17.5 MW. Plutonium is “Pu UOX” and its initial proportion is 3.7 mol% of heavy nuclei. The same library as for CANDU is used (ENDF/B-VI.8).

Unlike in our CANDU calculations, PWR assembly k_∞ is kept constant over a one-year cycle to a value related to core criticality (about 1.12). This is performed like in a real PWR, with no refueling during the cycle but by means of a predictor-corrector algorithm that regularly adjusts the natural boron concentration in water (initial concentration set to 2900 ppm).

Table 3: Simplified list of fission and "capture" (including all other absorptions) rates in initial Th/Pu CANDU bundle (for 1000 absorptions), compared to the Th/Pu PWR assembly.

	DRAGON		MURE		PWR	
	fission	capture	fission	capture	fission	capture
Th-232	5	307	5	308	7	159
Pu-238	0	9	0	10	2	6
Pu-239	301	140	299	138	281	157
Pu-240	1	79	1	79	5	160
Pu-241	90	30	89	30	92	29
Pu-242	0	7	0	7	1	26
water & O	-	6	-	9	-	15
boron	-	-	-	-	-	54
Zr & steel	-	25	-	25	-	6

In order to emphasize the main neutron economy differences between Th/Pu CANDU bundle and PWR assembly, Table 3 details how absorptions (excluding (n, xn) reactions) distribute in each case at start-up. The agreement between CANDU absorption balances is good despite the "water & O" term difference, due to the unavailability of O(n,α) data in the WLUP library.

From the same table, we can extract the instantaneous fissile Conversion Ratio (CR from now on) at a given time t, expressing the fuel self-sustainability in fissile nuclei by means of various reaction rates or macroscopic cross sections averaged over all fuel cells as defined here:

$$CR(t) = 1 - \frac{\Sigma_{capture}^{fertile} - \Sigma_{absorption}^{fissile}}{-\Sigma_{fission}^{total}} \tag{2}$$

where $\Sigma_{capture}^{fertile}$ stands for the production rate of fissile nuclei (U-233, Pu-239 and Pu-241) by capture on fertile isotopes (Th-232, Pu-238 and Pu-240) and $\Sigma_{absorption}^{fissile}$ stands for their consumption rate by absorption. $\Sigma_{fission}^{total}$ amounts simply to the total heavy nuclei consumption rate by fission. With BOC reaction rates of Table 3, we find $CR_{CANDU}^{BOC} = 1 - \frac{395-561}{-397} \simeq 0.58$ with DRAGON (0.60 with MURE). For the PWR Th/Pu assembly, CR_{PWR}^{BOC} = 0.40 only.

The main reasons for this are given again by Table 3. On one hand, the large boron reactivity reserve and the higher Pu concentration in PWR at BOC strongly reduces the absolute number of neutrons available for useful captures by fertile nuclei. On the other hand, the harder PWR spectrum (due to latter absorptions and to a less efficient moderator) makes capture-over-fission cross section ratios (known and designed from now on as α values) higher and therefore less propitious to high fissile conversion. By considering plutonium as the only fissile at start-up, we obtain $\alpha_{CANDU}^{BOC} \simeq 0.68$ with both methods. In comparison, α_{PWR}^{BOC} = 0.99, which shows that parasitic captures are more likely to be found in PWR. Likewise, we find α_{CANDU}^{EOC} = 0.67 (with α_{Pu} = 0.77 and α_{U-233} = 0.11), and α_{PWR}^{EOC} = 0.96 (with α_{Pu} = 1.03 and α_{U-233} = 0.16).

3.2.2 Inventory Comparison Over a Cycle

In Table 4, differences between methods can be easily noticed on important nuclei (mostly Th-232, Pa-233, U-233, U-236 and Pu-239) in the balance column. These can be imputed to slight modifications made in WLUP libraries compared to the basic ENDF data, such as pseudo fission products, simplified decay chains and omitted (n, xn) reactions. Another cause can be the different treatments of fission Q-values (as explained in part 3.1.2).

Table 4: Inventories at BOC and EOC of main actinides in CANDU Th/Pu bundle, given by DRAGON (EOC at t=170 days) and MURE (EOC at t=150 days). Balances normalized per GWe.y are compared with the one-year cycle PWR Th/Pu assembly (calculated by MURE).

	Mass (g) @ BOC	**Mass (g) @ EOC**		**Balance (kg/GWe.y)**		
		DRAGON	MURE	DRAGON	MURE	PWR
Th-232	17988	17921	17925	-913	-973	-517
Pa-231	0	0.171	0.181	2.33	2.79	3.86
Pa-233	0	15.7	16.3	214	252	44.8
U-232	0	0.0121	0.0115	0.16	0.18	0.52
U-233	0	44.7	40.6	609	627	383
U-234	0	1.26	1.15	17.2	17.7	17.9
U-235	0	0.034	0.031	0.46	0.48	1.41
U-236	0	0.0005	0.0025	0.006	0.038	0.13
Np-237	0	0.00032	0.00030	0.004	0.005	0.05
Pu-238	11.68	9.69	9.80	-27.1	-29.0	-24.8
Pu-239	198.6	122.6	127.2	-1036	-1103	-1221
Pu-240	93.05	99.85	99.59	92.7	101	-66.5
Pu-241	46.53	39.04	39.47	-102	-109	43.4
Pu-242	29.49	33.99	33.74	61.3	65.7	8.22
Am-241	0	0.81	0.73	11.1	11.3	45.2
Am-242m	0	0.0064	0.0047	0.088	0.072	0.83
Am-243	0	1.47	1.39	20.0	21.5	69.9
Cm-242	0	0.081	0.086	1.10	1.32	5.32
Cm-243	0	0.00035	0.00038	0.005	0.006	0.07
Cm-244	0	0.091	0.080	1.240	1.236	13.9

From BOC and EOC inventories, we deduce a global CR defined over each cycle by:

$$CR_{cycle} = 1 - \frac{\Delta FissileNucleiMass}{\Delta HeavyNucleiMass} \quad (3)$$

with Pa-233 counted as fissile, since after EOC all Pa-233 will decay in U-233. This gives a value of CR_{cycle}^{CANDU} = 0.70 for both MURE and DRAGON, while CR_{cycle}^{PWR} = 0.33 only. From a strictly scenario point of view, it means that contrary to Th/Pu PWRs, Th/Pu CANDUs could be symbiotically coupled to U/Pu fast breeders (with breeding ratio close to 1.3) [4]. Let us precise that PWRs and CANDUs are classical here, without any special modification. As expected, CANDU produces more U-233 (820 to 880 kg instead of only 430 kg/GWe.y of U-233 and Pa-233 for PWR) and less minor actinides. U-232 production by Pa-231(n,γ) allows related gamma detection in spent fuel (about 200 ppm of U-232 in U at EOC) against proliferation.

3.3 Comparison with a Heterogeneous Th+SEU Bundle

Slightly enriched uranium (SEU) can be used as a fissile starter. We choose a U-238/U-235 composition representative for cheap depleted uranium from spent PWR fuel (1.05 mol% of U-235). In order to minimize the SEU initial investment through the spectrum effect between rings, we dispose SEU pins in the most peripherical positions and pure ThO_2 pins at the center, as done in previous studies [3]. A satisfying starting point (k_∞ =1.13800 with DRAGON, 1.13840 with MURE) is found with the inner ring only (7 central pins) fueled with ThO_2.

With a $k_\infty^{threshold}$ evaluated to 1.045, burnup calculations give T_{cycle} = 380 days. This cycle is much longer than with Th/Pu fuel, thanks to the same Pu-239 effect that occurs in the U_{nat} bundle. This effect is nevertheless lower here, which explains that no real plutonium peak appears. The excellent agreement on T_{cycle} between our two codes can be explained by the very low influence of disturbing plutonium and heavier nuclei. Reactivity effects are logically found intermediate between U_{nat} and Th/Pu ones. Doppler ranges from about -0.9 pcm/K at BOC to 0.1 pcm/K at EOC, and CVR from about 700 pcm at BOC to 800 pcm at EOC. Finally, in Table 5 we compare Th/Pu and Th+SEU bundles in terms of U-233 production.

Table 5: Th/Pu and Th+SEU U-233 cycle productions, as calculated by DRAGON [MURE].

	Cycle time (days)	Cycle production (g/bundle) U-233	Pa-233	Total U-233 production after cooling (kg/GWe.y)
Th/Pu bundle	170 [150]	44.7 [40.6]	15.7 [16.3]	823 [879]
Th+SEU bundle	380 [380]	24.7 [25.2]	4.0 [4.2]	176 [180]

4. Conclusions and Perspectives

This work is based on the simple and convenient model of a mirrored CANDU-6 bundle, which is validated on the well-known U_{nat} case. A high level of confidence in our results has been gained by means of the systematic use of two independent methods; the deterministic code DRAGON and the C++ utility MURE based on the Monte Carlo code MCNP. These two codes are complementary, each having their strong points. MURE has for instance a more detailed nuclei chart, with all fission products explicit and direct use of ENDF data, but still uses some approximations like unique fission Q-value to be refined in the near future.

We have especially studied a homogeneous Th/Pu CANDU bundle, and compared it to a Th/Pu PWR assembly. Partly thanks to a softer spectrum and a reactivity management based on online refueling, CANDU can deal with short cycles, avoids the use of boron and has a higher fissile conversion ratio. We have observed that symbiotic scenarios between U/Pu fast breeders and Th/Pu classical CANDUs (but no Th/Pu classical PWRs) should be possible.

There is still a lot to do at the bundle level. The Th+SEU bundle is less U-233 productive than with Th/Pu, but seems more convenient to manage. Alternative options have to be investigated. The influence of the power level, related to the location in core, will be studied as well.

A mirrored assembly made of 3x3 bundles with the central one being thorium-fueled could then evaluate coupling effects between U_{nat} and thorium bundles that would occur in a partially thorium-loaded core. Such a method will certainly be useful to prepare real core studies, with precise online refueling schemes and detailed accidental transient safety simulations.

Acknowledgements

One of the authors (A.N.) acknowledges partial support from H. Nifenecker for his initial proposals and from D. Lecarpentier for his help on conversion ratio definitions. We are grateful to the AECL and LPSC Grenoble libraries for providing us kindly some needed reports. Finally, another author (G.M.) would like to acknowledge NSERC for its financial support.

References

1) K. Furukawa, A. Lecocq, Y. Kato and K. Mitachi, Thorium Molten-Salt Nuclear Energy Synergetics, Journal of Nucl. Sc. and Tech. Vol. 27, No. 12, 1157-1178 (1990).

2) L. Mathieu et al, Proposal for a Simplified TMSR, GLOBAL 2005 Proceedings, Tsukuba, Japan, October 9-13 (2005).

3) Thorium fuel utilization: options and trends, IAEA TECDOC 1319, IAEA Proceedings 1997-1999, http://www.iaea.org/inis/aws/fnss/abstracts/abst_te_1319_web.html.

4) E. Girardi and D. Lecarpentier, Symbiotic Pu/Thorium Fuel Cycle for HTGR, ENC 2005 Proceedings, Versailles, France, December 11-14 (2005).

5) F. Michel-Sendis et al, Plutonium Incineration and U-233 Production in Thorium Fueled Light Water Reactors, GLOBAL 2005 Proceedings, Tsukuba, Japan, October 9-13 (2005).

6) S. Şahin et al, An assessment of Thorium and spent LWR-fuel utilization potential in CANDU reactors, Energy Conversion and Management, 45, 1067-1085 (2004).

7) E. Critoph et al, Prospects for Self-Sufficient Equilibrium Thorium Cycles in CANDU Reactors, AECL-5501 (1976).

8) M.S. Milgram, Once-Through Thorium Cycles in CANDU Reactors, AECL-7516 (1982).

9) A. Hébert, G. Marleau and R. Roy, Application of the Lattice Code DRAGON to CANDU Analysis, Trans. Am. Nucl. Soc., 72, 335 (1995).

10) O. Méplan et al, MURE: MCNP Utility for Reactor Evolution, Description of Methods and First Applications, ENC 2005 Proceedings, Versailles, France, December 11-14 (2005).

11) J.F. Briesmeister, MCNP - a General Monte Carlo N Particle Transport Code, Version 4C, LANL, LA-13709-M (2000).

12) J. Griffiths, Reactor Physics and Economic Aspects of the CANDU Reactor System, a series of lectures presented in Indonesia, AECL-7615 (1981).

13) WIMS Library Update Project, http://www-nds.iaea.org/wimsd/index.html.

14) D. Rozon, Introduction à la cinétique des réacteurs nucléaires, Ecole Polytechnique de Montréal (1992).

15) B. Rouben, CANDU Fuel Management, Presentation at McMaster University (2003).

16) S. Sala, Réduction de la radiotoxicité des déchets nucléaires, Marseille I, thesis (1995).